A Member of the Dendritic Cell Family That Enters B Cell Follicles and Stimulates Primary Antibody Responses Identified by a Mannose Receptor Fusion Protein

By Claude Berney,* Suzanne Herren,* Christine A. Power,* Siamon Gordon,‡ Luisa Martinez-Pomares,‡ and Marie H. Kosco-Vilbois*

*From the *Serono Pharmaceutical Research Institute, CH-1228 Geneva, Switzerland; and the ‡Sir William Dunn School of Pathology, University of Oxford, Oxford OX1 3RE, United Kingdom*

Summary

Dendritic cells (DCs) are known to activate naive T cells to become effective helper cells. In addition, recent evidence suggests that DCs may influence naive B cells during the initial priming of antibody responses. In this study, using three-color confocal microscopy and three-dimensional immunohistograms, we have observed that in the first few days after a primary immunization, cells with dendritic morphology progressively localize within primary B cell follicles. These cells were identified by their ability to bind a fusion protein consisting of the terminal cysteine-rich portion of the mouse mannose receptor and the Fc portion of human immunoglobulin (Ig)G1 (CR-Fc). In situ, these CR-Fc binding cells express major histocompatibility complex class II, sialoadhesin, and CD11c and are negative for other markers identifying the myeloid DC lineage, such as (CD11b), macrophages (F4/80), follicular DCs (FDC-M2), B cells (B220), and T cells (CD4). Using CR-Fc binding capacity and flow cytometry, the cells were purified from the draining lymph nodes of mice 24 h after immunization. When injected into naive mice, these cells were able to prime T cells as well as induce production of antigen-specific IgM and IgG1. Furthermore, they produced significantly more of the lymphocyte chemoattractant, macrophage inflammatory protein (MIP)-1α, than isolated interdigitating cells. Taken together, these results provide evidence that a subset of DCs enters primary follicles, armed with the capacity to attract and provide antigenic stimulation for T and B lymphocytes.

Key words: dendritic cells • mannose receptor • antibody production • antigen presentation • chemokines

Antigen-specific lymphocytes, to initiate T cell–dependent antibody responses, must extravasate from the circulation into secondary lymphoid tissues, where they encounter signals for activation. Maturing dendritic cells (DCs)[1] migrate via blood or lymph into these organs and efficiently prime naive T cells (1, 2). This process involves the presentation of not only peptides but also costimulatory signals such as CD80 and CD86, the production of cytokines such as IL-12, and the release of chemokines such as IL-8, macrophage inflammatory protein (MIP)-1α, and MIP-1β (3–5).

Although much is known concerning DC–T cell interactions, it is only recently that investigators have found evidence that DCs may directly influence the production of antibody. Highly purified human $CD1a^+$ DCs have been shown to stimulate activated B cells to produce IgM and IgG in vitro (6). Furthermore, Wykes and colleagues have shown that rat DCs can transfer antigen to B cells and initiate a primary antibody response in vivo (7). Hence, it appears that DCs may have a broader role in lymphocyte activation than previously appreciated.

Studies performed by Kelsoe and colleagues originally suggested that early B cell activation occurs in the outer T cell zones of splenic periarteriolar sheaths (8–10). These foci were visualized due to the antigen-binding capacity of the B cells and, with time, contained an increased number of antigen-specific plasma cells. However, a recently published study using an adoptive transfer system of transgenic B and T cells has shown that early cognate interactions lo-

[1]*Abbreviations used in this paper:* BM-DC, bone marrow–derived DC; CR, cysteine-rich; 3D, three-dimension; DC, dendritic cell; FDC, follicular DC; MFI, mean fluorescence intensity; MIP, macrophage inflammatory protein; RANTES, regulated upon activation, normal T cell expressed and secreted.

 J. Exp. Med. © The Rockefeller University Press • 0022-1007/99/09/851/10 $5.00
Volume 190, Number 6, September 20, 1999 851–860
http://www.jem.org

calize to the follicular border in lymph nodes (11). The height of this interaction occurred at day 2–4 after immunization, suggesting that lymph node T and B cell priming events occur in these areas.

Previously in our laboratory, a chimeric protein was generated as a means to determine which cell types express ligands for the cysteine-rich (CR) domain of the murine mannose receptor (12). This chimera consisted of the CR domain of the mannose receptor fused to the Fc region of human IgG1 (CR-Fc). In conjunction with immunohistochemistry, the CR-Fc fusion protein revealed that cells with dendritic morphology accumulated in primary B cell follicles during the initial phases of an immune response while interdigitating cells in the paracortex remained negative (12). This observation was intriguing, leading us to develop methods to characterize this population in situ and ex vivo. The results reported here demonstrate that CR-Fc binding provides a marker for isolating a novel murine subset of $CD11c^+$ DCs that localize to B cell follicles and initiate humoral responses.

Materials and Methods

Animals and Immunizations. Female Balb/c mice were purchased from Janvier and kept under pathogen-free conditions. They were used at 8–12 wk of age. Mice were primed subcutaneously in each limb (50 μg) and in the back of the neck (100 μg) with chicken egg OVA (Sigma Chemical Co.) precipitated in alum (13).

Cryosections. Lymph nodes were obtained on days 0–4 after the primary immunization with OVA. Organs of a particular day were collected together and frozen in OCT compound on dry ice. The blocks were then cut into 10-μm-thick sections, air dried for 1 h, acetone fixed for 10 min, and finally stored at −20°C.

Generation of the CR-Fc Fusion Protein. The CR-Fc fusion protein was generated as described elsewhere (12). In brief, the CR domain of the mannose receptor was amplified by reverse transcription PCR and cloned into the pIG expression vector. The resulting plasmid was transfected into Cos-7 cells. The chimeric protein consisting of CR fused to the Fc portion of human IgG1 was purified from supernatants of transfected cells by protein A chromatography and stored at −20°C.

Immunohistochemistry. To characterize in situ the population binding the CR-Fc fusion protein, triple-color confocal microscopy was used. For this, CR-Fc binding cells were identified with Cy5 (λ_{em} = 670 nm), IgM^+ B cells with Texas red (λ_{em} = 615 nm), and a third protein with FITC (λ_{em} = 525 nm). These were excited with the 633- and 543-nm HeNe lasers and a 488-nm argon laser, respectively. This triple labeling then offered the most efficient strategy to (a) locate CR-Fc binding cells (blue) in relation to the IgM^+ B cell follicles (red); and then (b) determine if the blue cells expressed either a specific molecule or were adjacent to a certain cell type (green). The antibodies used for this third variable parameter included the following: N418 (anti-CD11c), M1/70 (anti-CD11b), 53-6.7 (anti-CD8α), T24 (anti-CD90/anti–Thy 1), GK 1.5 (anti-CD4), 14.8 (anti-B220), Syndecan-1 (anti-CD138), Ser-4/3D6 (antisialoadhesin), biotinylated FDC-M2 (anti-FDC), F4/80 (antimacrophage), biotinylated 14.4.4 (anti–MHC class II), and biotinylated NLDC-145 (anti-DEC205; a generous gift of K. Shortman, The Walter and Eliza Hall Institute of Medical Research, Melbourne, Australia). These mAbs, with the exception of NLDC-145, were either obtained from American Tissue Culture Collection and produced in house or, when available, purchased from PharMingen. Secondary antibodies and reagents included Texas red–conjugated rat anti–mouse IgM (Southern Biotechnology Associates), Cy5-conjugated mouse anti–human IgG (Jackson ImmunoResearch Laboratories), streptavidin-Cy5 (Caltag Laboratories), FITC-conjugated mouse anti–rat IgG (Southern Biotechnology Associates), FITC-conjugated mouse anti–rat IgG, FITC-conjugated mouse anti–human IgG (both from Jackson ImmunoResearch Laboratories), and FITC-conjugated goat anti–hamster IgG (Southern Biotechnology Associates). Human IgG (Jackson ImmunoResearch Laboratories) was used as a control for nonspecific binding of CR-Fc.

Three-dimension Immunohistograms. The photomicrographs were computer analyzed using a program developed in house. The program divides the image into 4,096 squares (64 × 64). The mean fluorescence intensity (MFI) is calculated for each of the squares and stored in a matrix. The MFI is then represented as a three-dimension (3D) histogram (x, y = position of the square, z = MFI). The 3D immunohistograms can represent single parameters as well as an overlay of two or more colors.

Isolation of CR-Fc Binding Cells. Mice were injected with OVA precipitated in alum (50 μg s.c. per limb and 100 μg s.c. behind the neck). 24 h later, the draining lymph nodes were collected and the cells recovered using an enzyme cocktail containing collagenase and DNAse (14). The low buoyant density cells (δ = 1.057–1.065 g/ml) were collected from Percoll gradients, and B cells were depleted with anti-B220–coated Dynabeads (Dynal). The remaining cells were sequentially incubated with CR-Fc (10 μg/ml) and N418 (10 μg/ml), biotinylated mouse anti–human IgG (1:100) and goat anti–hamster FITC (1:100; Southern Biotechnology Associates), and Streptavidin-PE (1:100; Serotec) before separation by flow cytometry. All washes and dilutions of reagents for FACS® used a solution consisting of PBS containing 10% FCS.

T Lymphocyte Priming In Vivo. For assessing in vivo T cell priming, the $N418^+$/CR-Fc binding cells were injected subcutaneously into the right side of naive mice. 7 d later, the draining (right side) and nondraining (left side) lymph nodes were collected separately, and the cells were recovered using the enzyme cocktail. The cells (obtained from the nondraining versus draining lymph nodes) were then fractionated using discontinuous Percoll gradients (15). The T cell band (δ = 1.081–1.085 g/ml) was collected and incubated with a cocktail of anti-CD8 (54.6.7), anti–MHC class II (14.4.4), and anti-B220 (14.8) coated Dynabeads according to the manufacturer's specifications. This method produced >98% $CD4^+$ T cells. The T cells (2×10^5 cells/well) were then incubated for 48 h in medium (IMDM, 5% FCS, l-glutamine, penicillin/streptomycin, and 2-ME) with spleen cells (irradiated with 30 Gy; 2×10^5 cells/well) in the presence or absence of 10 μg/ml OVA. For the final 24 h of culture, [^{3}H]thymidine was added and incorporation measured using a β-counter (Wallac).

T Lymphocyte Priming In Vitro. $N418^+$/CR-Fc binding cells were isolated as specified above and cultured overnight with T cells isolated from DO11.10 mice (i.e., transgenic for an OVA-specific T cell receptor [16]). At 24 h, [^{3}H]thymidine was added, and incorporation was measured 24 h later.

B Lymphocyte Priming In Vivo. For assessing in vivo B cell activation, both the $N418^+$/CR-Fc binding fraction and the

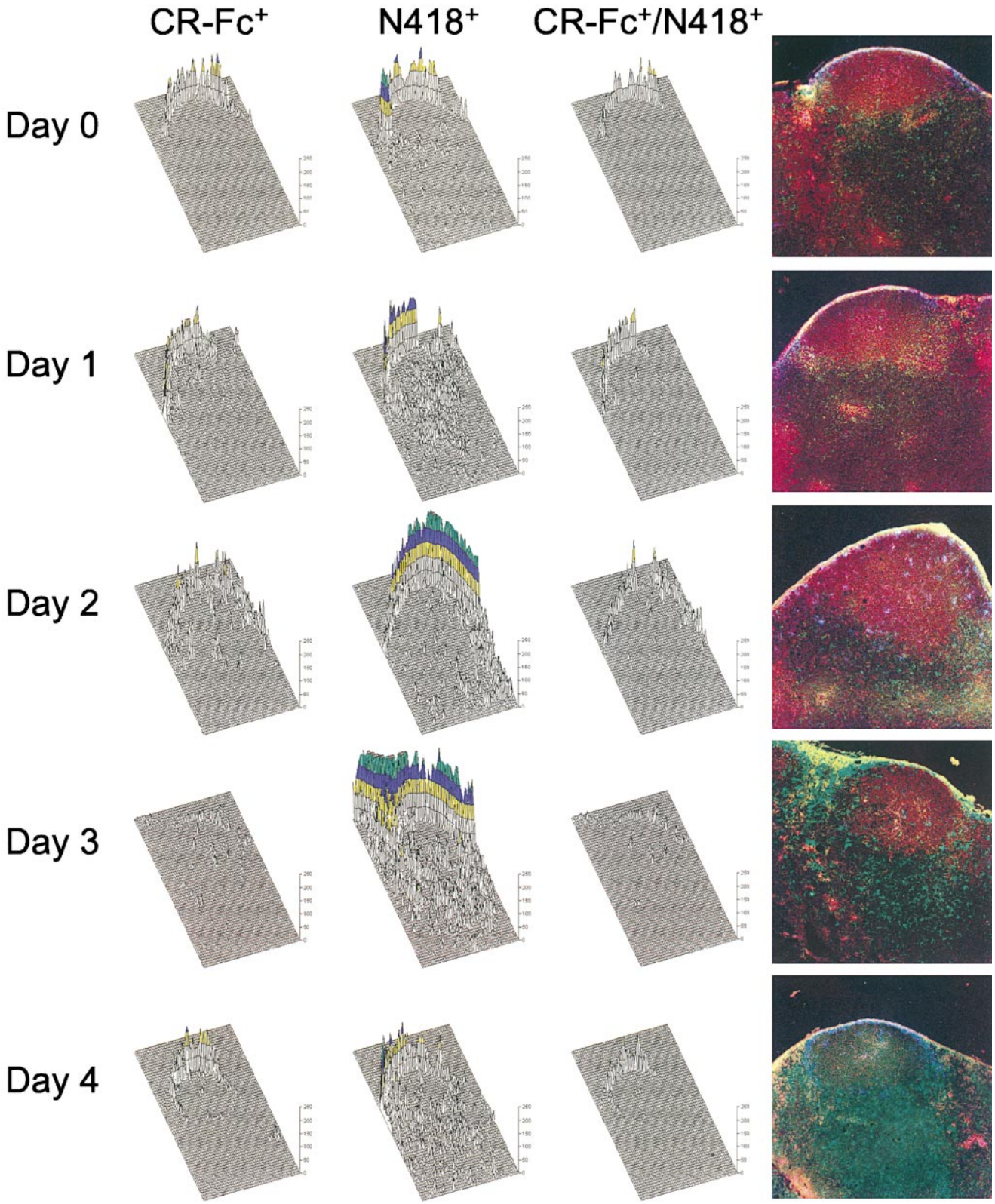

Figure 1. Localization of CR-Fc binding cells in lymph nodes with time after a primary immunization. Three-color confocal analysis was used in order to determine when and where CR-Fc binding cells appeared in the tissue. Cryostat sections prepared from murine lymph nodes obtained at days 0–4 (A–E) of a primary response were processed for IgM expression (red), N418 labeling (green), and CR-Fc binding (blue). The images were then digitally transformed using a computer program in order to map the MFI (in arbitrary units) for either single (CR-Fc$^+$; N418$^+$) or double (CR-Fc$^+$/ N418$^+$) positive cells. The resulting 3D immunohistograms revealed that CR-Fc binding cells accumulated with time in the outer part of the B cell follicles. Many of these cells were also N418$^+$ (see the CR-Fc$^+$/N418$^+$ column). The scale 0–250 represents the MFI, with the colors yellow, blue, green, and red representing values in the 100–150, 150–200, 200–250, and >250 range, respectively.

Table I. *Profile of CR-Fc$^+$ Cells in B Cell Follicles on Days 0, 1, 2, 3, and 4 of a Primary Immune Response*

Marker (mAb)	
CD11c (N418)	+
MHC class II (14.4.4)	+
Sialoadhesin (Ser-4/3D6)	+
F4/80 (F4/80)	−
CD11b (M1/70)	−
CD8α (53-6.7)	−/+*
Dec 205 (NLDC-145)	−
FDC-M2 (209)	−
CD90 (T24)	−/+*
CD4 (GK 1.5)	−
B220 (14.8)	−
CD138 (Syndecan-1)	−/+*

*A minor subset of cells was identified as positive on days 3 and 4.

N418$^+$/CR-Fc nonbinding population (representing interdigitating cells) were isolated as specified above. The CR-Fc binding cells were injected subcutaneously into the right forelimb while the CR-Fc nonbinding cells were injected subcutaneously into the left forelimb of naive mice. 7 d later, three sets of lymph nodes were collected and processed separately: (1) the draining lymph nodes receiving CR-Fc$^+$ cells (i.e., right axial and brachial), (2) the draining (i.e., left axial and brachial) lymph nodes receiving CR-Fc nonbinding cells, and (3) the lymph nodes receiving no cells (inguinal and paraaortic). Cells were recovered using the enzyme cocktail and fractionated using discontinuous Percoll gradients (15). The low buoyant density band (δ = 1.060–1.065 g/ml) was obtained and cultured for 1 h at 37°C to remove adherent cells. The nonadherent cells were then incubated (3×10^5 cells/well) in 96-well plates containing medium. After 7 d, the supernatants were collected, and OVA-specific antibody titers were assessed using standard ELISA procedures.

FACS® Analysis. The hybridomas 2.4G2 (anti-CD32) and YN1.1.7 (anti-CD54) were obtained from American Type Culture Collection, 7G6 (anti-CD21/35) from Dr. T. Kinoshita (Osaka University, Osaka, Japan), FGK (anti-CD40) from Dr. A. Rolink (Basel Institute for Immunology, Basel, Switzerland), and B3B4 (anti-CD23) from Dr. D. Conrad (Virginia Commonwealth University, Richmond, VA). 1G10 (anti-CD80), GL1 (anti-CD86), and 145-2c11 (anti-CD3) were purchased from PharMingen. The hybridoma Ser-4/3D6 (anti–mouse sialoadhesin) was generated in our laboratory. The secondary reagent was the mouse anti–rat IgG (H+L) F(ab′)$_2$ fragments conjugated to FITC (Jackson Immunoresearch Laboratories), and the control antibody, rat IgG, was purchased from Sigma Chemical Co.

Chemokine Production. N418$^+$/CR-Fc binding and N418$^+$/CR-Fc nonbinding cells were purified using flow cytometry according to the protocol mentioned above. In addition, DCs were derived from mouse bone marrow according to the protocol by Metlay et al. (17). In brief, the bone marrow was flushed from femurs, pipetted into a single cell suspension, and then incubated at 37°C, 5% CO_2 for 2 d in the presence of GM-CSF. At days 2 and 3, the nonadherent cells were removed after gentle pipetting, discarded, and new medium containing GM-CSF was added to the remaining adherent cells. On day 6, the nonadherent cells were harvested and shown to contain ≥99% N418$^+$ cells by flow cytometry. Cells were incubated at 37°C in 96-well plates (2×10^5 cells/well) in 200 μl IMDM plus 5% FCS (GIBCO BRL). Supernatants were harvested at 24 h, and chemokine levels were determined by ELISA using mouse-RANTES (kit MMR00; R&D Systems) and mouse–MIP-1α (kit MMA00; R&D Systems) kits according to the manufacturer's specifications.

Results

Determining the Phenotype In Situ of CR-Fc Binding Cells. During an immune response, it has been previously shown that within lymph nodes, cells with dendritic morphology bind the CR-Fc fusion protein (12). To further investigate their nature, we developed a system involving immunohistochemistry and three-color microscopy. As shown in Fig. 1, the B cell follicles were visualized using an anti-IgM antibody conjugated to Texas red. CR-Fc binding cells were labeled with Cy5-conjugated reagents. A third marker associated with FITC was then used to determine either the phenotype of the CR-Fc binding cells (double positive = cyan) or the proximity of these cells to other cell types. 3D histograms were then created in order to accurately assess the number and location of single or double positive cells.

The coexpression of the murine DC-specific marker, CD11c (using the N418 mab [17]), was assessed on lymph node sections obtained before (day 0) and 1, 2, 3, and 4 d after a primary immunization. In general, as shown in the histograms of Fig. 1, CR-Fc binding cells represented a subset of N418$^+$ cells. Before antigenic stimulation (Fig. 1, Day 0), no CR-Fc binding cells were observed below the subcapsular sinus. Within 24 h of antigen injection (Fig. 1, Day 1), CR-Fc single and CR-Fc/N418 double positive cells appeared in the follicle. By day 2, the cells were scattered throughout the follicle, becoming more organized towards the edge of the follicle during days 3 and 4. At day 5, very few CR-Fc/N418 double positive cells were observed except in the subcapsular sinus (data not shown).

As a control to address nonspecific Fc-mediated binding, the sections (days 0–3) were incubated with human IgG instead of the fusion protein CR-Fc. No binding was observed on the tissue sections (data not shown). Finally, very few, if any, N418$^+$ interdigitating cells in the paracortex demonstrated the ability to bind CR-Fc (Fig. 1).

Using this procedure, the expression of several proteins was analyzed (Table I). The CR-Fc binding cells in the follicles were observed to also express MHC class II and sialoadhesin, the latter being one of the ligands for CR-Fc (Martinez-Pomares, L., and S. Gordon, manuscript in preparation). A subset of cells expressed CD90 (Thy 1), especially the CR-Fc binding cells present at the border of the B cell follicle and paracortex. At days 3 and 4, a minor subset of cells also expressed CD8α and CD138 (Syndecan-1). However, CD11b, Dec205, CD4, FDC-M2, F4/80, and B220 were all absent. Taken together, these results re-

veal a novel pattern of protein expression for the CR-Fc binding cells that localize in B cell follicles.

CR-Fc Binding Cells Associate with B and T Lymphocytes in the Outer B Cell Follicles. Interestingly, many CR-Fc binding cells tended to localize at the border of the B cell follicle (Fig. 1). As it had recently been reported that adoptively transferred antigen-specific transgenic T and B cells colocalize in this region (11), we asked whether T cells could be observed in the vicinity of CR-Fc binding cells. As shown in Fig. 2 (see areas within boxes), indeed T cells ($CD4^+$) were found to be mingled with B cells (IgM^+) and CR-Fc binding cells at the periphery of the follicle between days 3 and 4 after antigen injection.

CR-Fc Binding Cells Prime T Cells In Vivo. The kinetics of their appearance in the particular anatomical location and their expression of the murine DC-specific protein, CD11c, suggested that CR-Fc binding cells play a role in lymphocyte stimulation. To address this hypothesis, CR-Fc

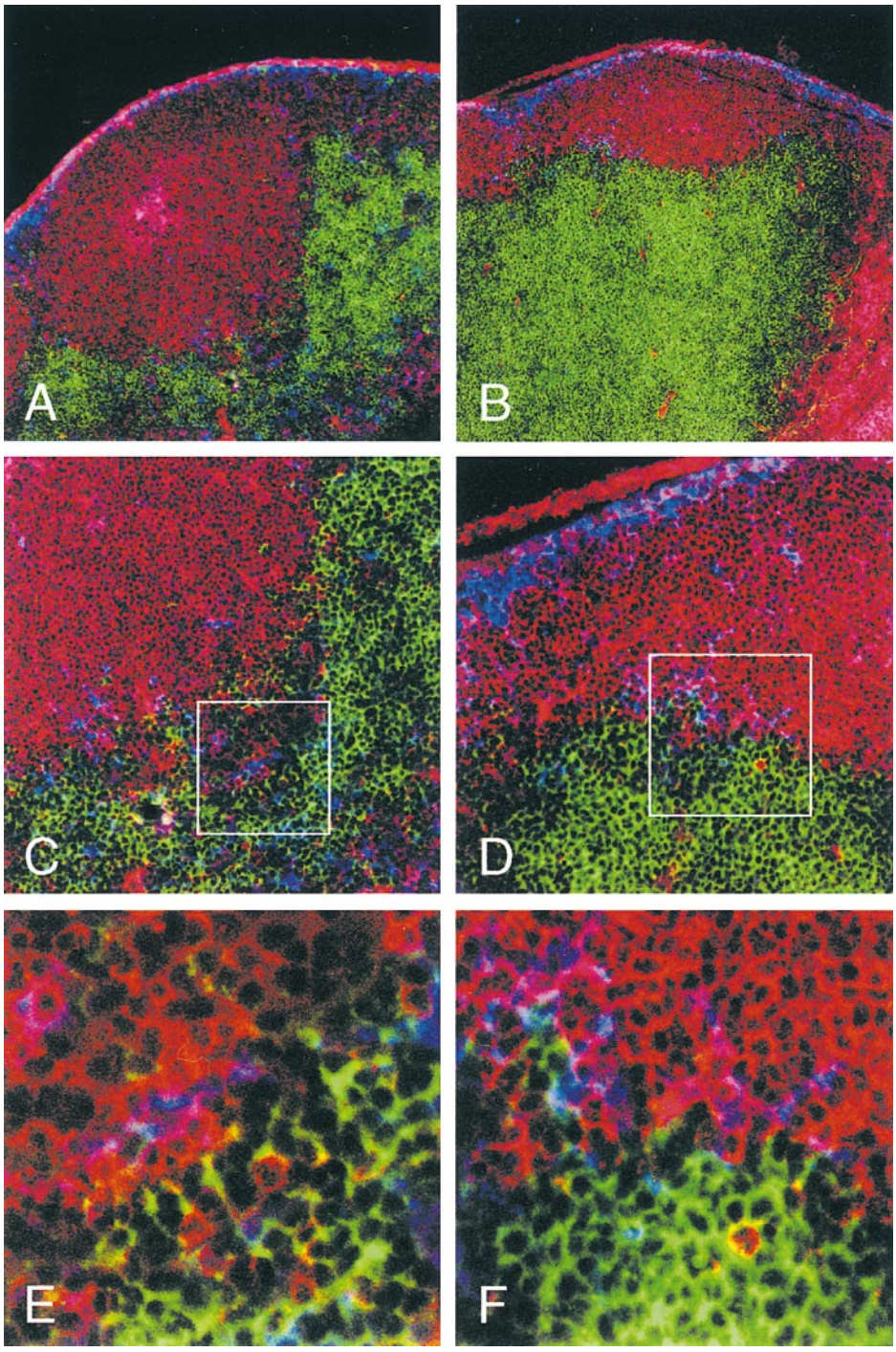

Figure 2. B cells, T cells, and CR-Fc binding cells colocalize in the outer B cell follicles. Cryostat sections prepared from murine lymph nodes obtained at day 3 (A, C, and E) and day 4 (B, D, and F) of a primary response were processed for IgM expression (red), CD4 labeling (green), and CR-Fc binding (blue). Especially at the higher magnification (E and F) of the areas outlined in C and D, CR-Fc binding cells (blue) and T cells (green) can be observed within the B cell follicles (red).

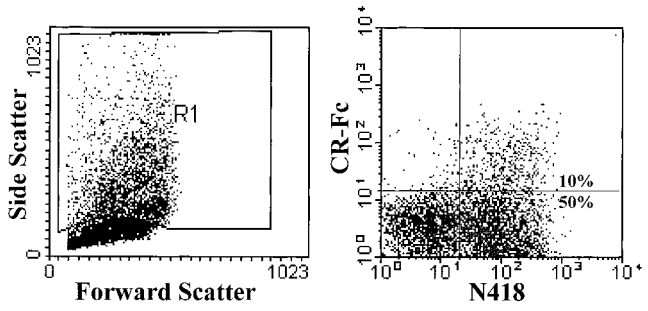

Figure 3. Profile of CR-Fc binding cells by flow cytometry. 24 h after a primary immunization, low buoyant density cells were labeled for CR-Fc binding and N418 expression. Setting a gate (R1) using the scatter parameters demonstrated that all $N418^+$ cells (gray) produced an elevated side scatter pattern. The N418 single positive cells represented 50% of the total low density population while 10% were N418/CR-Fc double positive.

binding cells were isolated from draining lymph nodes 24 h after subcutaneous injection of OVA and purified by flow cytometry. As shown in Fig. 3, the CR-Fc binding cells had a high side scatter value and were all $CD11c^+$. Sorting the CR-Fc binding cells using the R1 gate (Fig. 3) produced a purity of >99%.

The cells were then adoptively transferred into naive mice, and 7 d later, the T cells were isolated separately from the draining versus nondraining lymph nodes. As shown in Fig. 4 A, the CR-Fc binding cells were able to prime naive T cells, as no antigen-specific proliferation occurred in T cells isolated from the nondraining side. These results suggested that CR-Fc binding cells were capable of antigen uptake in vivo followed by processing and presentation of peptides to naive T cells.

CR-Fc Binding Cells Present Antigen to T Cells In Vitro. To insure that CR-Fc binding cells could present antigen they obtained in vivo, the cells, isolated in a similar manner as above, were incubated in decreasing concentrations with antigen-specific T cells. As few as 3,000 CR-Fc binding cells (Fig. 4 B) were able to significantly stimulate the DO11.10 transgenic T cells to proliferate in vitro. Therefore, not only can CR-Fc binding cells take up antigen in vivo, they can also act as antigen-presenting cells both in vitro and in vivo.

CR-Fc Binding Cells Induce Antigen-specific Antibody Production by B Cells. As B cells are stimulated to produce the initial wave of antigen-specific Ig in the outer T cell zones, an experiment was designed to ascertain if CR-Fc binding cells played a role in this process. Similar to the protocol mentioned above, CR-Fc binding cells were isolated from draining lymph nodes 24 h after a subcutaneous injection of OVA. In addition, CR-Fc nonbinding cells were also obtained for comparison. The CR-Fc binding cells were then adoptively transferred into the right forelimb of naive mice while the CR-Fc nonbinding cells were injected into the left. 7 d later, the B cells were isolated separately from the right versus left axillary and brachial lymph nodes as well as the inguinal and paraaortic lymph nodes (i.e., the sites receiving no cells). They were then cultured for a further 7 d, at which time the supernatants were harvested. As shown in Fig. 5, only cells isolated from lymph nodes receiving the CR-Fc binding cells produced antigen-specific antibody. Although only a remote possibility due to the 24-h time point used for isolation, contamination by preplasma cells in the CR-Fc preparations was ruled out by putting these cells in culture for 7 d and assaying for antibody production by ELISA (none was detected; data not shown). In addition, the same results as shown in Fig. 5 were obtained when CR-Fc binding preparations were subjected to a round of B220 depletion using magnetic beads before injection into mice (data not shown).

Next, to determine the characteristics of the antigen-specific antibody response in vivo after transfer of CR-Fc

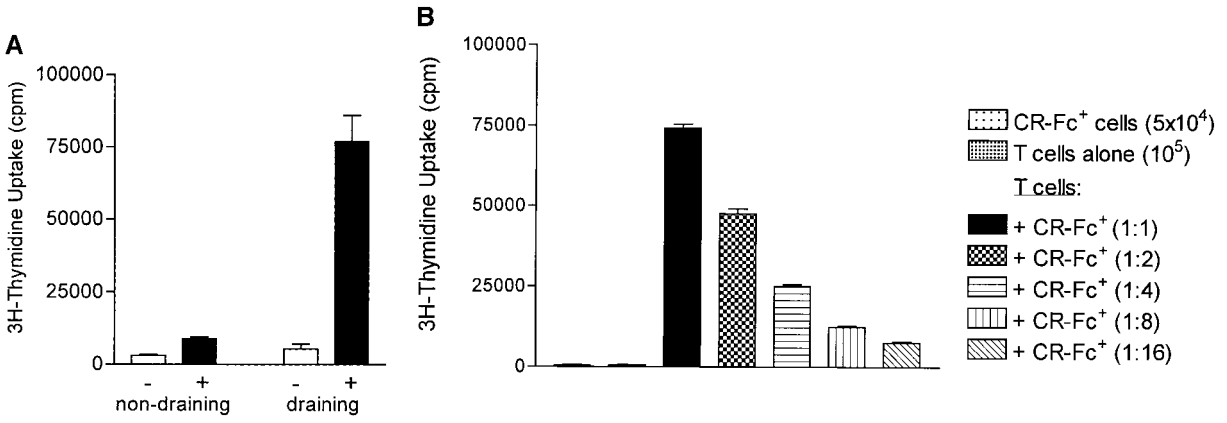

Figure 4. T cell priming by CR-Fc binding cells. (A) CR-Fc binding cells were isolated from OVA-immune mice, then injected subcutaneously into naive mice. 7 d later, the T cells were isolated from the lymph nodes on the side receiving the injection and compared with T cells isolated from nondraining lymph nodes for in vitro restimulation. In the presence of splenic antigen-presenting cells, both T cell populations were incubated without (−) or with (+) OVA. At 24 h, [3H]thymidine was added, and 24 h later, incorporation was assessed. (B) CR-Fc binding cells were isolated from immune mice and then incubated at varying concentrations with 10^5 OVA-specific transgenic T cells. At 24 h, [3H]thymidine was added, and 24 h later, incorporation was assessed. Both sets of data are representative of three experiments.

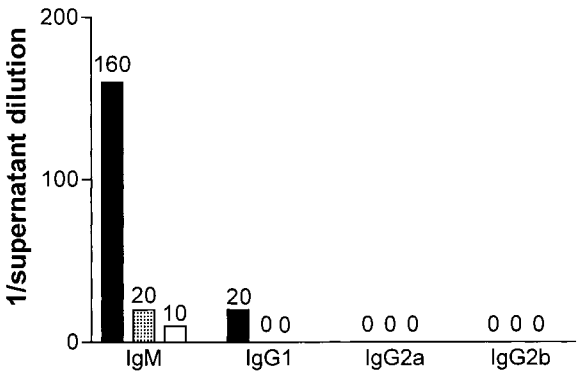

Figure 5. OVA-specific antibody titers in B cell supernatants from the lymph nodes of mice receiving CR-Fc binding versus nonbinding or no cells. CR-Fc binding and nonbinding cells were isolated from OVA-immune mice, then injected subcutaneously into naive mice. 7 d later, the B cells were isolated from the lymph nodes on the side receiving CR-Fc binding (black bars) or nonbinding (stippled bars) cells. In addition, B cells from lymph nodes draining sites where no cells were injected were also evaluated (white bars). The B cells were cultured for 7 d, and then the supernatants were subjected to ELISA to determine the level of isotype-specific anti-OVA titers. The data are presented as the maximum dilution at which a titer was still observed. These data are representative of five experiments.

binding cells, serum was collected from mice after a single and second injection of cells. As shown in Fig. 6, a significant increase was observed for OVA-specific IgG1 titers after both the primary and secondary injections. IgM did not increase, although this was clearly observed when B cells were assessed ex vivo (as in Fig. 5). These data suggest that although the B cells that encounter CR-Fc cells can become IgM-secreting cells ex vivo, left in vivo, they will encounter signals that drive IgG1 production and can be induced to produce an increased level of antibody after a secondary application of the stimulus. IgG2a and IgG2b antigen-specific serum titers showed a slight but not statistically significant change. This observation suggests that transfer of CR-Fc cells themselves does not promote the development of microenvironments for downstream Ig class switching events.

Cell Surface Molecules Expressed by Isolated CR-Fc Binding DCs. Double immunolabeling in conjunction with flow cytometry revealed that the CR-Fc binding cells were rich in Fc (CD32) and complement (CD21/35) receptors (Fig. 7). In addition, they were positive for intercellular adhesion molecule 1 (ICAM-1, CD54), CD40, and CD86 (B7-2) whereas they expressed little to no CD80 (B7-1). The cells also expressed sialoadhesin (Ser-4/3D6), one of the ligands for CR-Fc. Finally, neither CD3 nor CD23 were expressed.

CR-Fc Binding Cells Differ from Interdigitating Cells and Bone Marrow–derived DCs in Their Ability to Produce MIP-1α. $N418^+$/CR-Fc nonbinding cells (i.e., interdigitating cells) and $N418^+$/CR-Fc binding cells isolated 24 h after antigen injection as well as $N418^+$ DCs derived from bone marrow (BM-DCs) were assessed for their capacity to produce T cell chemoattractants. As shown in Fig. 8, RANTES (for regulated upon activation, normal T cell expressed and secreted) production followed the hierarchy of BM-DC $<$ CR-Fc^+/$N418^+$ $\leq$ CR-Fc^-/$N418^+$ (interdigitating cell). In contrast, only $N418^+$/CR-Fc binding cells produced MIP-1α.

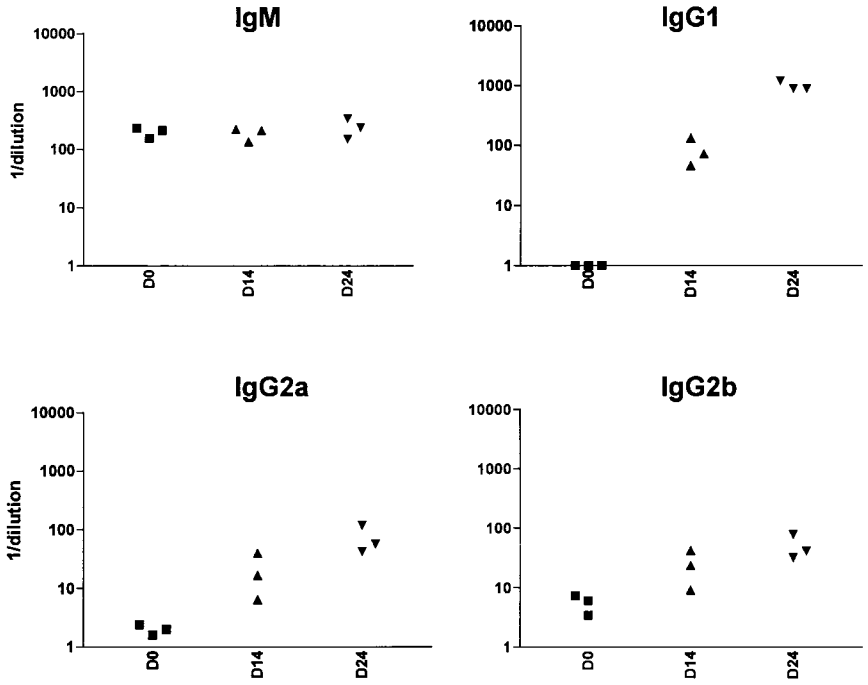

Figure 6. OVA-specific serum titers of mice receiving CR-Fc binding cells. CR-Fc binding cells were isolated from OVA-immune mice, then adoptively transferred subcutaneously into naive mice (10^5 per mouse). 14 d later, the same mice were injected subcutaneously a second time with a freshly isolated preparation of CR-Fc binding cells from OVA-immune mice (5×10^4 per mouse). Serum was obtained before the primary (D0) and secondary (D14) injections. Isotype-specific anti-OVA titers were assessed by ELISA. Each data point represents the maximum dilution at which a titer was still observed for an individual mouse.

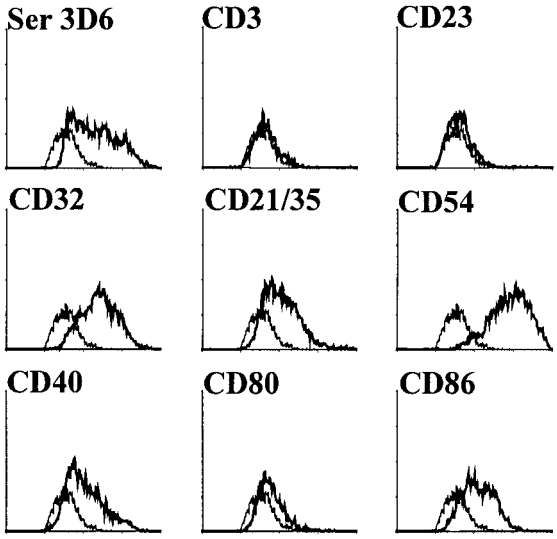

Figure 7. Cell surface molecules expressed by isolated CR-Fc binding cells. CR-Fc binding cells were isolated 24 h after OVA injection. The cells were then double labeled for CR-Fc plus one of the markers indicated. The fine line represents the level of fluorescence of CR-Fc binding cells with a control antibody, and the bold line represents the level of expression on CR-Fc binding cells of the specific marker.

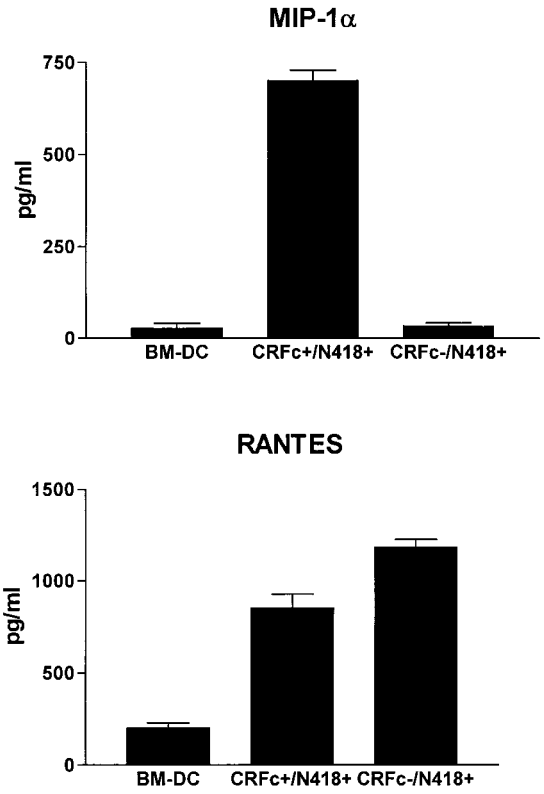

Figure 8. Chemokine production by the different subsets of DC. Day 6 BM-DCs, CR-Fc binding cells (CR-Fc$^+$/N418$^+$; isolated 24 h after OVA injection), and interdigitating cells (CR-Fc$^-$/N418$^+$; isolated 24 h after OVA injection) were isolated and cultured for 24 h in medium. Supernatants were then harvested, and the levels of MIP-1α and RANTES were determined by ELISA.

Discussion

Using the CR-Fc binding property, we have identified a population of cells that localize within B cell follicles. These cells appear to be members of the DC family, as they express CD11c in situ and ex vivo and are capable of priming naive T cells. Whether the cells belong to the myeloid or lymphoid lineage is unclear, as CD11b and DEC205, proteins normally associated with the myeloid and lymphoid DC lineage, respectively, were not detected. The lack of F4/80, CD4, and FDC-M2 expression, molecules found on macrophages (18), germinal center DCs (19), and FDCs (20), respectively, further define these as a unique DC subset.

As CR-Fc binding DCs appear mainly in the follicles and not the paracortex, these cells may represent a population specifically suited to precipitating the early phases of humoral immunity. These cells provoke antigen-specific antibody responses in vivo after adoptive transfer, and the isotypes (i.e., IgM and IgG1) produced are restricted to that associated with initial antibody responses (8, 9). These data together with the in vitro and in vivo T cell priming results are significant because they suggest that CR-Fc binding cells have a mechanism not only for presenting peptide but also for transporting native antigen to the B cell compartment. Our observations concur with those of Wykes and colleagues, who showed that DCs can capture and retain unprocessed antigen in vitro and in vivo and could transfer this antigen to naive B cells to initiate specific antibody responses (7). This mechanism would provide an efficient means of initiating early protective immunity when physiological (i.e., low) doses of virus or bacteria enter the body and are encountered by the sentinel DCs. Indeed, low affinity polyclonal IgM is essential for the resistance of mice to a systemic bacterial infection (21). Hence, DCs moving in from the blood or interstitial sites, quickly providing both peptide and native antigen for lymphocyte stimulation in microenvironments of secondary lymphoid tissues, would prove to be evolutionarily advantageous for survival.

The functional profile of these murine-derived CR-Fc binding DCs parallels that of the human CD14$^+$-derived DCs characterized by Caux and colleagues (22). The CD14$^+$-derived DCs have a robust and long-lasting antigen uptake capacity (22) resulting in the induction of efficient T cell proliferation, and demonstrate a unique ability to induce naive B cell differentiation into IgM-secreting plasma cells. In addition, the accessory molecule profiles of the murine and human DC subtypes are similar, as only CD40 and CD86 are necessary for CD14$^+$-derived DC–induced T cell proliferation while CD80 plays no role. As shown in Fig. 7, the murine CR-Fc binding DC expresses CD40 and CD86 but is negative for CD80.

Assessing the chemokine production by various murine DC subsets demonstrated that CR-Fc binding DCs have a unique phenotype compared with immature (day 6) BM-DCs and interdigitating cells (the remaining population of CD11c$^+$ lymph node cells isolated 24 h after antigen injec-

tion). Although the significance of a more robust MIP-1α production remains to be shown, this may relate to the CR-Fc binding DC ability to recruit cell types quickly into the tissue (23). MIP-1α is reported to attract both T cells and other DCs (24, 25). Furthermore, MIP-1α may also act as a B cell chemoattractant, as B cells have been shown to express mRNA for CC chemokine receptor CCR1 (26, 27). As other reagents become available to determine the levels of murine chemokine production, we will be able to further define the function of this cell type during immune responses.

Is the CR-Fc binding DC a migratory cell, or are we witnessing upregulation of a receptor on a resident population? Based on the ability of the CR-Fc binding DCs to prime naive T cells in lymph nodes after a subcutaneous adoptive transfer as well as their similarity to human $CD14^+$-derived DCs, we favor the former. The relationship of the murine CR-Fc binding DC to the germinal center DC remains to be further investigated. In the future, the use of imaging systems as described by Robert and colleagues (28) should provide the means to trace the exact fate of CR-Fc binding cells in vivo.

We would like to thank Dr. Jean Pierre Aubry for expertise during the initial phases of this work, and Chris Hebert for production of the artwork.

Address correspondence to Marie H. Kosco-Vilbois, Serono Pharmaceutical Research Institute, 14, chemin des Aulx, CH-1228 Geneva, Switzerland. Phone: 41-22-706-9708; Fax: 41-22-794-6965; E-mail: marie.kosco-vilbois@serono.com

Submitted: 1 March 1999 Revised: 12 July 1999 Accepted: 13 July 1999

References

1. Steinman, R.M., M. Pack, and K. Inaba. 1997. Dendritic cells in the T cell areas of lymphoid organs. *Immunol. Rev.* 156:25–38.
2. Banchereau, J., and R.M. Steinman. 1998. Dendritic cells and the control of immunity. *Nature.* 392:245–252.
3. Caux, C., C. Massacrier, B. Vanbervliet, B. Dubois, C. Van Kooten, I. Durand, and J. Banchereau. 1994. Activation of human dendritic cells through CD40 cross-linking. *J. Exp. Med.* 180:1263–1272.
4. Cella, M., D. Scheidegger, K. Palmer-Lehmann, P. Lane, A. Lanzavecchia, and G. Alber. 1996. Ligation of CD40 on dendritic cells triggers production of high levels of interleukin-12 and enhances T cell stimulatory capacity: T–T help via APC activation. *J. Exp. Med.* 184:747–752.
5. Koch, F., U. Stanzl, P. Jennewein, K. Janke, C. Heufler, E. Kampgen, N. Romani, and G. Schuler. 1996. High level IL-12 production by murine dendritic cells: upregulation via MHC class II and CD40 molecules and downregulation by IL-4 and IL-10. *J. Exp. Med.* 184:741–746.
6. Dubois, B., B. Vanbervliet, J. Fayette, C. Massacrier, C. Van Kooten, F. Briere, J. Banchereau, and C. Caux. 1997. Dendritic cells enhance growth and differentiation of CD40-activated B lymphocytes. *J. Exp. Med.* 185:941–951.
7. Wykes, M., A. Pombo, C. Jenkins, and G. MacPherson. 1998. Dendritic cells interact directly with naive B lymphocytes to transfer antigen and initiate class switching in a primary T-dependent response. *J. Immunol.* 161:1313–1319.
8. Jacob, J., R. Kassir, and G. Kelsoe. 1991. In situ studies of the primary immune response to (4-hydroxy-3-nitrophenyl)acetyl. I. The architecture and dynamics of responding cell populations. *J. Exp. Med.* 173:1165–1175.
9. Jacob, J., and G. Kelsoe. 1992. In situ studies of the primary immune response to (4-hydroxy-3-nitrophenyl)acetyl. II. A common clonal origin for periarteriolar lymphoid sheath–associated foci and germinal centers. *J. Exp. Med.* 176:679–687.
10. Kelsoe, G. 1995. In situ studies of the germinal center reaction. *Adv. Immunol.* 60:267–288.
11. Garside, P., E. Ingulli, R.R. Merica, J.G. Johnson, R.J. Noelle, and M.K. Jenkins. 1998. Visualization of specific B and T lymphocyte interactions in the lymph node. *Science.* 281: 96–99.
12. Martinez-Pomares, L., M. Kosco-Vilbois, E. Darley, P. Tree, S. Herren, J.Y. Bonnefoy, and S. Gordon. 1996. Fc chimeric protein containing the cysteine-rich domain of the murine mannose receptor binds to macrophages from splenic marginal zone and lymph node subcapsular sinus and to germinal centers. *J. Exp. Med.* 184:1927–1937.
13. Gray, D., M. Kosco, and B. Stockinger. 1991. Novel pathways of antigen presentation for the maintenance of memory. *Int. Immunol.* 3:141–148.
14. Kosco, M.H., E. Pflugfelder, and D. Gray. 1992. Follicular dendritic cell-dependent adhesion and proliferation of B cells in vitro. *J. Immunol.* 148:2331–2339.
15. Kosco-Vilbois, M.H., D. Gray, D. Scheidegger, and M. Julius. 1993. Follicular dendritic cells help resting B cells to become effective antigen-presenting cells: induction of B7/BB1 and upregulation of major histocompatibility complex class II molecules. *J. Exp. Med.* 178:2055–2066.
16. Murphy, K.M., A.B. Heimberger, and D.Y. Loh. 1990. Induction by antigen of intrathymic apoptosis of CD4+ CD8+TCRlo thymocytes in vivo. *Science.* 250:1720–1723.
17. Metlay, J.P., M.D. Witmer-Pack, R. Agger, M.T. Crowley, D. Lawless, and R.M. Steinman. 1990. The distinct leukocyte integrins of mouse spleen dendritic cells as identified with new hamster monoclonal antibodies. *J. Exp. Med.* 171: 1753–1771.
18. Austyn, J.M., and S. Gordon. 1981. F4/80, a monoclonal antibody directed specifically against the mouse macrophage. *Eur. J. Immunol.* 11:805–815.
19. Grouard, G., I. Durand, L. Filgueira, J. Banchereau, and Y.J.

Liu. 1996. Dendritic cells capable of stimulating T cells in germinal centres. *Nature*. 384:364–367.
20. Kosco-Vilbois, M.H., H. Zentgraf, J. Gerdes, and J.Y. Bonnefoy. 1996. To "B" or not to "B" a germinal center? *Immunol. Today*. 18:225–230.
21. Boes, M., A.P. Prodeus, T. Schmidt, M.C. Carroll, and J. Chen. 1998. A critical role of natural immunoglobulin M in immediate defense against systemic bacterial infection. *J. Exp. Med*. 188:2381–2386.
22. Caux, C., B. Vanbervliet, C. Massacrier, D. Dezutter-Dambuyant, B. de Saint-Vis, C. Jacquet, K. Yoneda, S. Imamura, D. Schmitt, and J. Banchereau. 1996. $CD34^+$ hematopoietic progenitors from human cord blood differentiate along two independent dendritic cell pathways in response to GM-CSF+TNF alpha. *J. Exp. Med*. 184:695–706.
23. Sallusto, F., and A. Lanzavecchia. 1999. Mobilizing dendritic cells for tolerance, priming, and chronic inflammation. *J. Exp. Med*. 189:611–614.
24. Gao, J.L., D.B. Kuhns, H.L. Tiffany, D. McDermott, X. Li, U. Francke, and P.M. Murphy. 1993. Structure and functional expression of the human macrophage inflammatory protein 1 alpha/RANTES receptor. *J. Exp. Med*. 177:1421–1427.
25. Sozzani, S., F. Sallusto, W. Luini, D. Zhou, L. Piemonti, P. Allavena, J. Van Damme, S. Valitutti, A. Lanzavecchia, and A. Mantovani. 1995. Migration of dendritic cells in response to formyl peptides, C5a, and a distinct set of chemokines. *J. Immunol*. 155:3292–3295.
26. Sharma, V., D. Walper, and R. Deckert. 1997. Modulation of macrophage inflammatory protein-1alpha and its receptors in human B-cell lines derived from patients with acquired immunodeficiency syndrome and Burkitt's lymphoma. *Biochem. Biophys. Res. Commun*. 235:576–581.
27. Schall, T.J., K. Bacon, R.D. Camp, J.W. Kaspari, and D.V. Goeddel. 1993. Human macrophage inflammatory protein α (MIP-1α) and MIP-1β chemokines attract distinct populations of lymphocytes. *J. Exp. Med*. 177:1821–1826.
28. Robert, C., J.D. Fuhlbrigge, J.D. Kieffer, S. Ayehunie, R.O. Hynes, G. Cheng, S. Grabbe, U.H. von Adrian, and T.S. Kupper. 1999. Interaction of dendritic cells with skin endothelium: a new perspective on immunosurveillance. *J. Exp. Med*. 189:627–635.